IEEE Access
Multidisciplinary ⋮ Rapid Review ⋮ Open Access Journal

Received December 15, 2019, accepted January 2, 2020, date of publication January 6, 2020, date of current version January 16, 2020.

Digital Object Identifier 10.1109/ACCESS.2020.2964265

Semi-Globally Practical Finite-Time H_∞ Control of TCSC Model of Power Systems Based on Dynamic Surface Control

LING CHANG[1,2], YANG LIU[3], YUANWEI JING[1], XIANGYONG CHEN[4,5], AND JIANLONG QIU[4,5], (Member, IEEE)

[1]College of Information Science and Engineering, Northeastern University, Shenyang 110819, China
[2]Faculty of Information and Control Engineering, Shenyang Urban Construction University, Shenyang 110167, China
[3]School of Automation, Guangdong University of Technology, Guangzhou 510006, China
[4]School of Automation and Electrical Engineering, Linyi University, Linyi 216000, China
[5]Key Laboratory of Complex Systems and Intelligent Computing, Linyi University, Linyi 216000, China

Corresponding authors: Yuanwei Jing (ywjjing@mail.neu.edu.cn) and Xiangyong Chen (cxy8305@163.com)

This work was supported in part by the Postdoctoral Science Foundation under Grant 2019M662812, and in part by the National Natural Science Funds of China under Grant 61773108 and Grant 61903092.

ABSTRACT A less-complex semi-globally practical finite-time stability (SGPFS) result is presented for thyristor-controlled series compensation (TCSC) model of the power system by using dynamic surface control (DSC), H_∞ control and prescribed performance control (PPC) in this paper. Meanwhile, a set of preassigned finite-time functions (PFTF) are chosen. The designed controller makes the rotor angle converge to a predefined arbitrary small area within a finite-time interval and other states of the closed-loop system are bounded. In addition, the proposed design method is simpler and the presented result is also easier to be achieved. Finally, simulation results are given to verify the effectiveness and superiority of the theoretical finding.

INDEX TERMS Power systems, TCSC, semi-globally practical finite-time control, dynamic surface control, H_∞ theory.

I. INTRODUCTION

A. REVIEW AND INSPIRATION

As a representative device of flexible AC transmission systems, the control study of the thyristor controlled series compensation (TCSC) has received significant attention due to its transient stability enhancement, damping control and voltage regulation. The merit of TCSC, as shown in [1], lies in that it can not only improve the stability of the power system during a process of the long-distance transmission, but also reduce transmission line's equivalent electric distance. Based on the advantages, numerous researchers devote to design the corresponding controller for TCSC from a wide range of objectives and a large number of profound results have also been achieved. In [2], TCSC controllers are designed by using the linear matrix inequality (LMI) to achieve the coordination of multi-machine, and a optimization algorithm is employed to minimize the H_∞ norm. Authors in [3] and [4] investigate the stability problem for TCSC with the help of the frequency domain method and linear quadratic gaussian (LQG) technique, respectively. But, the above-discussed results are obtained by virtue of the linearization model ignoring the nonlinear nature. As a result, the passivity control, prefeedback and Hamiltonian method are combined to improve stability of the nonlinear power system in [5]. Together with Minimax and adaptive backstepping schemes, authors of [6] develop a disturbance attenuation controller for TSCS model. In [7], a nonlinear PI adaptive controller is designed for TCSC. A modified harmony search method is adopted to design a coordinate TCSC and power system stability (PSS) controllers in [8] where the interaction of controllers with the aid of minimizing the objective function is improved. Based on the chaotic optimization theory, a fuzzy controller is introduced for the model of TCSC in [9], in which only the local signal is utilized rather than wide area signal. Recently, some novel control algorithms are presented in [10]–[12].

The associate editor coordinating the review of this manuscript and approving it for publication was Dongbo Zhao.

In [10], a new design scheme is given for multi-machine power systems together with the nonlinear TCSC controller by using the zero dynamic technique. The design problem of the sliding mode controller is addressed in [11] along with a disrupted oppositional learned gravitational search algorithm. Under the actuator saturation, a wide-area robust control method is discussed in [12] for TCSC to ensure that the damping of the oscillation among areas can be enhanced.

On the other hand, during the past decades, the finite-time control (FTC) of nonlinear systems has become an exciting research field. A great deal of results have also been achieved (see [13]–[18] and references therein) where various nonlinear systems are included such as strict-feedback systems, non-strict feedback systems, stochastic systems, switched systems etc. FTC has been also widely applied to numerous fields such as spacecraft, underwater vehicles, bank-to-turn missiles, mobile robots and network systems, to just name a few. It is interesting that these results are obtained based on three sufficient conditions, that is, $\dot{V}(t) + c_1 V^\alpha(t) \leq 0$, $\dot{V}(t) + c_1 V^\alpha(t) + c_2 V(t) \leq 0$ or $\dot{V} \leq -c_1 V^\alpha + b$ with $c_1 > 0$, $c_2 > 0$, $b > 0$ and $0 < \alpha < 1$. Moreover, most of designed ideas are achieved via an ''adding power integration'' (API) technique proposed in [19] by Lin et al. But, the API method makes the design process of finite-time controllers very sophisticated, which limits the application of FTC to some extent. It is worth noting that an obvious merit in [20] and [21] is its simplicity. However, only local finite-time results are obtained owing to the utilization of a homogeneous approximation, and the considered nonlinear systems must be homogeneous. [22] and [23] propose a simpler finite-time controller design procedure for nonlinear systems and high-order multi-agent systems by employing a time-varying scaling function, respectively. However, up to now, there have been a few research papers which focus on simplifying finite-time design process. Therefore, it is still an open area and necessary to be further investigated.

As is well known, the dynamic surface control (DSC) (see [24]–[27] and references therein) can be used to address the problem of ''explosion of complexity'' of backstepping. With the help of DSC, repeated differentiations with respect to virtual control laws are eliminated, which results in a simpler design process. Besides, another control method called prescribed performance control (PPC) (see [28]–[31] and references therein) compels the output tracking error to remain a predefined region all the time. Meanwhile, the error trajectory converges to an arbitrary small zone at steady state by choosing an appropriate performance function and an error transformation function. However, it is worth emphasizing that all the performance functions in [29]–[31] attenuate to a preset area in infinite-time.

Note that a simple design process and a low-complexity compute are very necessary during the controller process, however, the existing methods for the considered power system exist two problems. On one hand, the issue on the ''explosion of terms' caused by backstepping technique [6], [7] increases the computational burden of control method. On the other hand, the existing practical finite-time approaches need multiple inequality amplification [14]–[16], which results in a large control input. In view of the above cases, this paper considers to use DSC scheme to reduce computational burden of the presented design method. Meanwhile, a novel finite-time design idea is introduced to simplify design process of the existing methods. Due to that the external disturbances are inevitable, an effective robust control technique, that is, H_∞ control, is combined in this work. To the best of authors'knowledge, thus far, there is no reported research about the semi-globally practical finite-time stability (SGPFS) for TCSC by means of PPC, DSC and H_∞ control. Inspired by some preliminary results in the design of TCSC and nonlinear finite-time controllers, a challenging problem is to be considered, namely, *how to simplify an SGPFS controller design process for TCSC power system via DSC and PPC.*

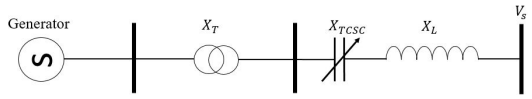

FIGURE 1. A single-machine infinite-bus system with TCSC.

B. MAIN CONTRIBUTIONS OF THIS WORK

A single-machine infinite-bus system with TCSC shown in Fig. 1 and the model of TCSC system is described by the following state space form [5].

$$\begin{aligned}
\dot{\delta} &= \omega_s \omega \\
\dot{\omega} &= \frac{1}{M}\left(P_m - D\omega - E_q^{'} V_s y_{\text{tcsc}} \sin\delta\right) + d_1 \\
\dot{y}_{\text{tcsc}} &= \frac{1}{T_{\text{tcsc}}}\left(u - y_{\text{tcsc}} + y_{\text{tcsc0}}\right) + d_2 \\
y &= \begin{bmatrix} q_1\delta \\ q_2\omega \end{bmatrix}^{\text{T}}
\end{aligned} \tag{1}$$

where δ, ω and M are the rotor angle, the rotor speed, the inertial coefficient of the generator, respectively. y_{tcscs} is the admittance with $y_{\text{tcsc}} = \frac{1}{X_{d\Sigma}^{'} - X_{\text{tcsc}}}$ and y_{tcsc0} being the steady value of y_{tcsc}. D is the damping coefficient. X_{tcsc} is equivalent reactance of TCSC and $X_{d\Sigma}^{'} = X_d^{'} + X_T + X_L$ is the external perimysium reactance with $X_d^{'}$, X_T and X_L being the transient reactance of generator d-axis, transformer reactance and transmission line reactance, respectively. ω_s represents the synchronous angular velocity. $E_q^{'}$, V_s, P_m and T_{tcsc} denote the q-axis transient potential, the infinite bus voltage, the mechanical power of the prime motor and the inertia time constant of TCSC, respectively. $u \in R$ stands for the control input. y is the output with q_1 and q_2 being the nonnegative constant. $d = [d_1, d_2]^{\text{T}}$ denotes the external disturbances.

The novelties and contributions are listed as follows:

1) This paper is the first attempt to provide a less-complex finite-time controller design procedure with API, PPC and DSC, which is also used to address the finite-time control

problem for power systems for the first time. It should be pointed out that the dynamic surface control, practical finite-time control and H_∞ theory are employed to address "explosion of complexity", finite-time convergence and external disturbances, respectively. As a result, the control objective cannot be simultaneously achieved by only utilizing single technique.

2) A novel sufficient condition for SGPFS is given to guarantee that the generator rotor angle converges to a prescribed area in finite-time in this work, which is different from that in [2]–[5], [5]–[12].

3) In contrast to [13]–[15], the settling time is independent of design parameters and initial conditions, and the presented finite-time control law is smooth, which guarantees that the solution to the closed-loop system is unique.

4) A recursive process is employed to design a SGPFS controller, which ensures that the influence of disturbances on the output of TCSC is attenuated up to a given degree.

The rest of this paper is organized as follows. Section II states some useful definitions and lemmas. A model transformation is constructed in III. Then, the main result of this work is shown in Section IV. In Section V, the stability analysis is given. Section VI demonstrates simulation results. Finally, the conclusion is summarized in Section VII.

II. PROBLEM STATEMENT AND PRELIMINARIES

The control objectives of this paper are that a less-complexity controller is designed to ensure that i) the generator rotor angle converges to a predefined region within a finite-time interval and satisfies the corresponding transient and steady-state performances; and ii) all the signals of the closed-loop system are bounded; iii) when the disturbances are zero, the output of the system is bounded, when they are not equal to zero, the following inequality holds.

$$\int_0^t \|y\|^2 dt \leq \varsigma \int_0^t \|d\|^2 dt + \upsilon \tag{2}$$

with ς and υ being two positive constants. To achieve the above objectives, the following definition is given first.

Definition 1 ([32], [33]): A smooth function $\rho(t)$ is called a preassigned finite-time function (PFTF), if it $\bigoplus$ satisfies three properties: 1) $\rho(t) > 0$; 2) $\dot{\rho}(t) \leq 0$; 3) $\lim_{t\to T_f} \rho(t) = \rho_{T_f} > 0$ and $\rho(t) = \rho_{T_f}$ for any $t \geq T_f$ with ρ_{T_f} and T_f being the arbitrarily small constant and the settling time, respectively.

In this work, a PFTF is defined by (3).

$$\rho(t) = \begin{cases} \left(\rho_0 - \frac{t}{T_f}\right) e^{\left(1-\frac{T_f}{T_f - t}\right)} + \rho_{T_f}, & t \in [0, T_f) \\ \rho_{T_f}, & t \in [T_f, +\infty) \end{cases} \tag{3}$$

with $\rho_0 > \frac{5}{4}$ and $\rho_{T_f} > 0$.

Remark 1: It is worth noting that (3) satisfies all the properties mentioned in Definition 1. Moreover, $\rho(0) = \rho_0 + \rho_{T_f}$ is the initial value of $\rho(t)$, and $\lim_{t\to T_f} \rho(t) = \rho_{T_f}$. Besides, the proof of the smoothness of $\rho(t)$ can be found in [32] and [33].

Remark 2: Performance functions $\rho(t)$ possess the property of finite-time convergence, however, the conventional performance functions (4) and (5) (see [29], [30] and [31]) do not have this property, which is a key difference between (3) and (4)-(5).

$$\rho_1(t) = (\rho_0 - \rho_\infty) e^{-\theta t} + \rho_\infty \tag{4}$$

$$\rho_2(t) = \coth(\mu t + \iota) - 1 + \rho_\infty \tag{5}$$

where ρ_0, ρ_∞, θ, μ and ι are positive design parameters.

Next, transformation functions are chosen as

$$S(\varepsilon) = \frac{e^{\varepsilon} - e^{-\varepsilon}}{e^{\varepsilon} + e^{-\varepsilon}} \tag{6}$$

where ε represents the transformed error.

Remark 3: It is easy to know that $S(\varepsilon)$ possesses the following properties: 1) it is a smooth and strictly increasing function; 2) $S(\varepsilon) \in (-1, 1)$; 3) $\lim_{\varepsilon\to+\infty} S(\varepsilon) = 1$ and $\lim_{\varepsilon\to-\infty} S(\varepsilon) = -1$.

In order to achieve the objective i), the following equality is made.

$$\delta = \rho(t) S(\varepsilon), \quad i = 1, \cdots, n \tag{7}$$

Remark 4: It follows from $-1 < S(\varepsilon) < 1$ and $\rho(t) > 0$ that $-\rho(t) < \rho(t)S(\varepsilon) < \rho(t)$ holds, which results in $-\rho(t) < \delta < \rho(t)$. Hence, the generator rotor angle δ can be restrained in $(-\rho(t), \rho(t))$ if and only if ε is bounded. In addition, due to the decreasing performance of $\rho(t)$, δ will be confined within the following set during a finite-time interval.

$$\Delta = \{\delta \in R : |\delta| \leq \rho_{i,T_f}, t \geq T_f\} \tag{8}$$

which explains that the objective i) is achieved.

Next, to obtain the main result, the following definition and lemmas are given.

Definition 2 ([18]): Consider a nonlinear system (9).

$$\dot{x} = f(x) \tag{9}$$

with x being a state vector. It is assumed that $f(x) : \Omega \to R^n$ is continuous on an open neighbourhood Ω of the origin with $f(0) = 0$. If there are $\varsigma > 0$ and $0 < T(x_0) < \infty$ for each initial condition $x(0) = x_0$ such that the following inequality holds

$$\|x(t)\| \leq \varsigma, \quad t \geq T$$

where $T(x_0)$ denotes a settling time, then the origin of system (9) is called to be semi-globally practical finite-time stable (SGPFS).

Lemma 1 ([18]): The trajectory of system (9) is SGPFS, if there exist a C^1 function $V(x) > 0$ with $V(0) = 0$ and three positive numbers $m > 0$, $0 < \zeta < 1$ and $0 < \Xi < \infty$ such that

$$\dot{V}(x) + mV^{\zeta}(x) \leq \Xi \tag{10}$$

where $V(x)$ is defined on a neighbourhood $U \subset R^n$ of the origin.

III. MODEL TRANSFORMATION

Before giving the transformed model, the TCSC model (1) can be rewritten as (11) with $x_1 = \delta$, $x_2 = \omega$ and $x_3 = y_{\text{tcsc}}$.

$$\begin{aligned} \dot{x}_1 &= h_1 x_2 + f_1 \\ \dot{x}_2 &= h_2 x_3 + \theta x_2 + f_2 + d_1 \\ \dot{x}_3 &= h_3 u + f_3 + d_2 \\ y &= \begin{bmatrix} q_1 x_1 \\ q_2 x_2 \end{bmatrix}^{\mathrm{T}} \end{aligned} \tag{11}$$

where $h_1 = \omega_s$, $h_2 = -\frac{1}{M} E_q^{'} V_s \sin x_1$, $h_3 = \frac{1}{T_{\text{tcsc}}}$, $f_1 = 0$, $f_2 = \frac{1}{M} P_m$, $f_3 = -\frac{1}{T_{\text{tcsc}}} (x_3 - x_{30})$ and $\theta = -\frac{D}{M}$ is unknown parameter due to the existence of unknown parameter D. Moreover, θ is estimated online.

It is worth noting that $\sin x_1 \neq 0$ when the system is running stably. Therefore, a new model with respect to variable ε will be established in this section. In view of (7), one has

$$\dot{x}_1 = \dot{\rho}(t) S(\varepsilon) + \rho(t) \frac{\partial S(\varepsilon)}{\partial \varepsilon} \dot{\varepsilon}(t) \tag{12}$$

From (7), (11) and (12), it is easy to know that (13) holds.

$$\dot{\varepsilon} = \frac{h_1 x_2 + f_1 - \dot{\rho}(t) S(\varepsilon)}{\rho(t) \frac{\partial S(\varepsilon)}{\partial \varepsilon}} = \bar{h}_1 x_2 + \bar{f}_1 \tag{13}$$

where $\bar{h}_1 = \frac{h_1}{\rho(t) \frac{\partial S(\varepsilon)}{\partial \varepsilon}}$ and $\bar{f}_1 = \frac{f_1 - \dot{\rho}(t) S(\varepsilon)}{\rho(t) \frac{\partial S(\varepsilon)}{\partial \varepsilon}}$.

Then, (11) is rewritten as the following form.

$$\begin{aligned} \dot{\varepsilon} &= \bar{h}_1 x_2 + \bar{f}_1 \\ \dot{x}_2 &= h_2 x_3 + \theta x_2 + f_2 + d_1 \\ \dot{x}_3 &= h_3 u + f_3 + d_2 \\ y &= \begin{bmatrix} q_1 x_1 \\ q_2 x_2 \end{bmatrix}^{\mathrm{T}} \end{aligned} \tag{14}$$

IV. SEMI-GLOBALLY PRACTICAL FINITE-TIME CONTROLLER DESIGN FOR TCSC

In this section, a semi-globally practical finite-time controller will be designed and the whole controller design process contains the following three steps. First, a set of dynamic surfaces are given by (15).

$$\begin{aligned} z_1 &= \varepsilon \\ z_2 &= x_2 - s_1 \\ z_3 &= x_3 - s_2 \end{aligned} \tag{15}$$

where s_i, $i = 1, 2$, are the output of the filter introduced in the sequel.

Step 1: Differentiating z_1 with respect to time yields

$$\dot{z}_1 = \bar{h}_1 x_2 + \bar{f}_1 \tag{16}$$

The virtual controller law is chosen as

$$\alpha_1 = -\frac{1}{\bar{h}_1} \left(k_1 z_1 + \bar{f}_1 + \frac{1}{2} \bar{h}_1^2 z_1 \right) \tag{17}$$

where $k_1 > 0$ is a design parameter. It is well known that the backstepping design method is subject to the issue of "explosion of terms". Hence, in order to avoid it, the following low-pass filter with a time constant τ_1 is employed.

$$\tau_1 \dot{s}_1 + s_1 = \alpha_1, s_1(0) = \alpha_1(0) \tag{18}$$

Step 2: Taking the time derivative of z_2 gives

$$\begin{aligned} \dot{z}_2 &= \dot{x}_2 - \dot{s}_1 \\ &= h_2 x_3 + \theta x_2 + f_2 + d_1 - \frac{\alpha_1 - s_1}{\tau_1} \\ &= h_2 z_3 + h_2 s_2 + \theta (z_2 + s_1) + f_2 + d_1 - \frac{\alpha_1 - s_1}{\tau_1} \end{aligned} \tag{19}$$

A virtual controller α_2 is taken as

$$\alpha_2 = -\frac{1}{h_2} \left[k_2 z_2 + \frac{z_2}{4\gamma_1^2} + \frac{1}{2} h_2^2 z_2 + \hat{\theta} (z_2 + s_1) - \frac{\alpha_1 - s_1}{\tau_1} + f_2 + \bar{h}_1 z_1 \right] \tag{20}$$

where $k_2 > 0$ and $\gamma_1 > 0$ represent the design parameters, $\hat{\theta}$ is the estimation of θ.

Similar to Step 1, a low-pass filter with a time constant τ_2 is selected as (21).

$$\tau_2 \dot{s}_2 + s_2 = \alpha_2, \quad s_2(0) = \alpha_2(0) \tag{21}$$

Step 3: In the same way, $\dot{z}_3$ can be written as

$$\dot{z}_3 = \dot{x}_3 - \dot{s}_2 = h_3 u + f_3 + d_2 - \frac{\alpha_2 - s_2}{\tau_2} \tag{22}$$

It follows that the real controller in Step 3 can be selected by (23).

$$u = -\frac{1}{h_3} \left(k_3 z_3 - \frac{\alpha_2 - s_2}{\tau_2} + \frac{z_3}{4\gamma_2^2} + f_3 + h_2 z_2 \right) \tag{23}$$

Remark 5: It follows from Section III that $\bar{h}_1 \neq 0$ and $h_i \neq 0$ with $i = 2, 3$. As a consequence, the functions in (17), (20) and (23) are well defined.

Remark 6: An important advantage of dynamic surface control (DSC) is to avoid "explosion of terms" caused by backstepping technique. For some low-order systems, such as first-order or second-order systems, it is indeed not necessary to use DSC, however, the considered single-machine system is third-order system. Although it is not very complex, the utilization of DSC can indeed reduce computational burden. Because if DSC technique is employed during the controller design, then $\dot{\alpha}_1$ needs to be calculated by

$$\begin{aligned} \dot{\alpha}_1 = {} & \frac{\partial \alpha_1}{\partial z_1} \left(\frac{\partial \alpha_1}{\partial x_1} \dot{x}_1 + \frac{\partial \alpha_1}{\partial \rho} \dot{\rho} \right) \\ & + \frac{\partial \alpha_1}{\partial \bar{h}_1} \left[\frac{\partial \bar{h}_1}{\partial \rho} \dot{\rho} + \frac{\partial \bar{h}_1}{\partial \left(\frac{\partial S(\varepsilon)}{\partial \varepsilon} \right)} \frac{\partial S^2(\varepsilon)}{\partial \varepsilon^2} \right] \\ & + \frac{\partial \alpha_1}{\partial \bar{f}_1} \left[\frac{\partial \bar{f}_1}{\partial \rho} \dot{\rho} + \frac{\partial \bar{f}_1}{\partial S(\varepsilon)} \dot{S}(\varepsilon) + \frac{\partial \bar{f}_1}{\partial \left(\frac{\partial S(\varepsilon)}{\partial \varepsilon} \right)} \frac{\partial S^2(\varepsilon)}{\partial \varepsilon^2} \right] \end{aligned}$$

from which, it is a little difficult to compute the derivative of α_1. In addition, the derivative of α_2 will be more complicated due to calculation of $\dot{\alpha}_1$. As a result, it is necessary to utilize DSC to simplify the design process.

V. STABILITY ANALYSIS

The stability analysis of the closed-loop system is carried out and the main result is given in this section. First, a set of boundary layer errors are defined by

$$e_i = s_i - \alpha_i, \quad i = 1, 2 \tag{24}$$

According to (15)-(17) and (24), (25) holds. Together with (15) (19), (20) and (24), (26) holds. Similarly, (27) holds by combining with (15) and (22)-(24).

$$\dot{z}_1 = -k_1 z_1 + \bar{h}_1 z_2 + \bar{h}_1 e_1 - \frac{1}{2}\bar{h}_1^2 z_1 \tag{25}$$

$$\dot{z}_2 = -k_2 z_2 - \bar{h}_1 z_1 - \frac{1}{2}h_2^2 z_2 - \frac{z_2}{4\gamma_1^2} + \tilde{\theta}\left(z_2 + s_1\right) + h_2\left(z_3 + e_2\right) + d_1 \tag{26}$$

$$\dot{z}_3 = -k_3 z_3 - h_2 z_2 - \frac{z_3}{4\gamma_2^2} + d_2 \tag{27}$$

and boundary layer errors $\dot{e}_1$ and $\dot{e}_2$ can be rewritten as

$$\dot{e}_1 = -\frac{e_1}{\tau_1} + \Omega_1\left(z_1, z_2, \rho, \dot{\rho}, \ddot{\rho}\right) \tag{28}$$

$$\dot{e}_2 = -\frac{e_2}{\tau_2} + \Omega_2\left(z_1, z_2, z_3, \rho, \dot{\rho}, \cdots, \rho^{(4)}\right) \tag{29}$$

where $\Omega_1(\cdot)$ and $\Omega_2(\cdot)$ represent the derivative of the virtual controller α_1 and α_2. Moreover, it is easily seen that they are continuous functions.

Next, the main result of this paper is given by choosing a Lyapunov function V

$$V = \sum_{i=1}^{3}\frac{1}{2}z_i^2 + \sum_{i=1}^{2}\frac{1}{2}e_i^2 + \frac{1}{2\mu}\tilde{\theta}^2 \tag{30}$$

where $\tilde{\theta} = \theta - \hat{\theta}$ with $\hat{\theta}$ being the estimation of θ.

Taking the time derivative of the Lyapunov function V produces

$$\begin{aligned}\dot{V} &= z_1\dot{z}_1 + z_2\dot{z}_2 + z_3\dot{z}_3 + e_1\dot{e}_1 + e_2\dot{e}_2 - \frac{1}{\mu}\tilde{\theta}\dot{\hat{\theta}} \\ &= -k_1 z_1^2 - k_2 z_2^2 - k_3 z_3^2 + \bar{h}_1 z_1 e_1 + h_2 z_2 e_2 \\ &\quad - \frac{z_2^2}{4\gamma_1^2} - \frac{z_3^2}{4\gamma_2^2} + z_2 d_1 + z_3 d_2 \\ &\quad - \frac{e_1^2}{\tau_1} - \frac{e_2^2}{\tau_2} + e_1\Omega_1 + e_2\Omega_2 \\ &\quad - \frac{1}{2}\bar{h}_1^2 z_1^2 - \frac{1}{2}h_2^2 z_2^2 \\ &\quad - \frac{1}{\mu}\tilde{\theta}\left[\dot{\hat{\theta}} - z_2\left(z_2 + s_1\right)\mu\right]\end{aligned}$$

Due to the following inequalities

$$\begin{aligned}\bar{h}_1 z_1 e_1 &\le \frac{1}{2}\bar{h}_1^2 z_1^2 + \frac{1}{2}e_1^2 \\ h_2 z_2 e_2 &\le \frac{1}{2}h_2^2 z_2^2 + \frac{1}{2}e_2^2 \\ z_2 d_1 &= -\left\|\frac{z_2}{2\gamma_1} - \gamma_1 d_1\right\|^2 + \frac{z_2^2}{4\gamma_1^2} + \gamma_1\left\|d_1\right\|^2 \\ &\le \frac{z_2^2}{4\gamma_1^2} + \gamma_1\left\|d_1\right\|^2 \\ z_3 d_2 &= -\left\|\frac{z_3}{2\gamma_2} - \gamma_2 d_2\right\|^2 + \frac{z_3^2}{4\gamma_2^2} + \gamma_2\left\|d_2\right\|^2 \\ &\le \frac{z_3^2}{4\gamma_2^2} + \gamma_2\left\|d_2\right\|^2\end{aligned}$$

Then, $\dot{V}$ can be rewritten as

$$\begin{aligned}\dot{V} \le &-\sum_{i=1}^{3}k_i z_i^2 + \frac{1}{2}e_1^2 + \frac{1}{2}e_2^2 - \frac{1}{\mu}\left[\dot{\hat{\theta}} - z_2\left(z_2 + s_1\right)\mu\right] \\ &+ \gamma_1\left\|d_1\right\|^2 + \gamma_2\left\|d_2\right\|^2 - \frac{e_1^2}{\tau_1} - \frac{e_2^2}{\tau_2} + e_1\Omega_1 + e_2\Omega_2\end{aligned} \tag{31}$$

For any given p, define a compact set

$$\Phi = \left\{\left[\bar{z}^{\mathrm{T}} + \bar{e}^{\mathrm{T}} + \hat{\theta}^{\mathrm{T}}\right]^{\mathrm{T}} : V \le p\right\} \subset \mathbb{R}^5$$

with $\bar{z} = [z_1, z_2, z_3]^{\mathrm{T}}$ and $\bar{e} = [e_1, e_2]^{\mathrm{T}}$. Therefore, there exist $Q_i > 0$ such that $|\Omega_i(\cdot)| \le Q_i$ on the set Φ because of the continuity of $\Omega_i(\cdot)$ with $i = 1, 2$. According to Young's inequality, (31) becomes

$$\dot{V} \le -\sum_{i=1}^{3}k_i z_i^2 - \sum_{i=1}^{2}\left(\frac{1}{\tau_i} - 1\right)e_i^2 + \Theta + \varsigma\left(\left\|d_1\right\|^2 + \left\|d_2\right\|^2\right) \tag{32}$$

with $\Theta = \sum_{i=1}^{2}\frac{1}{2}Q_i^2$, $k_i > 0$, $0 < \tau_i < 1$, $\gamma = \max\{\gamma_1, \gamma_2\}$ and the adaptive law is defined by

$$\dot{\hat{\theta}} = z_2\left(z_2 + s_1\right)\mu - \varkappa\hat{\theta} \tag{33}$$

It follows from (30) and (32) that (34) holds.

$$\dot{V} \le -2\lambda V + \bar{\Theta} + \gamma\left(\left\|d_1\right\|^2 + \left\|d_2\right\|^2\right) \tag{34}$$

with $\bar{\Theta} = \Theta + \frac{\varkappa}{2\mu}\hat{\theta}^2$, $\lambda = \min\left\{2k_i, 2\left(\frac{1}{\tau_j} - 1\right), \frac{\varkappa}{2\mu}\right\}$, $i = 1, 2, 3$ and $j = 1, 2$.

Case 1: The disturbances are equal to zero, that is, $d_1 = d_2 = 0$. Integrating (34) on $[0, t]$ produces

$$0 \le V \le \frac{\bar{\Theta}}{2\lambda} + V(0)\, e^{-2\lambda t} \tag{35}$$

which results in that all the signals z_i and e_j, $i = 1, 2, 3$, $j = 1, 2$ are bounded. It follows from (17) and (24) that α_1 and s_1 are bounded. Due to the boundedness of s_1 and z_2, x_2 is bounded. In the similar way, it can be inferred that α_2, s_2 and u are bounded. In addition, it can be concluded that the state

x_1 converge to the predefined zone by means of finite-time performance functions $\rho(t)$ in (3) and state transformations in (7).

Case 2: When $d_1 \neq 0$ and $d_2 \neq 0$, (32) can be rewritten as

$$V(t) - V(0) \leq \int_0^t \left[-k_1 z_1^2 - k_2 z_2^2 + \bar{\Theta} + \gamma\left(\|d_1\|^2 + \|d_2\|^2\right)\right] dt \quad (36)$$

which implies that

$$\int_0^t \left(k_1 z_1^2 + k_2 z_2^2\right) dt \leq \gamma \int_0^t \|d\|^2 dt + \tilde{\Theta} \quad (37)$$

with $\tilde{\Theta} = V(0) + \bar{\Theta}$. In order to verify (2) holds, it is first to explain that $q_1^2 x_1^2 \leq k_1 z_1^2$ and $q_2^2 x_2^2 \leq k_2 z_2^2$. It follows from (7) and $S^2(\varepsilon) \leq \varepsilon^2$ that $q_1^2 x_1^2 \leq q_1^2 \rho_0^2 \varepsilon^2 = q_1^2 \rho_0^2 z_1^2 \leq k_1 z_1^2$ if and only if $q_1^2 \rho_0^2 \leq k_1$. Similarly,

$$\begin{aligned} q_2^2 x_2^2 - k_2 z_2^2 &= q_2^2 x_2^2 - k_2 (x_2 - s_1)^2 \\ &= q_2^2 x_2^2 - k_2 x_2^2 - k_2 s_1^2 + 2k_2 x_2 s_1 \\ &\leq q_2^2 x_2^2 - k_2 x_2^2 - k_2 s_1^2 + k_2^2 s_1^2 + x_2^2 \\ &= \left(q_2^2 - k_2 + 1\right) x_2^2 + \left(k_2^2 - k_2\right) s_1^2 \end{aligned}$$

which indicates that $q_2^2 x_2^2 \leq k_2 z_2^2$ if and only if $q_2^2 - k_2 + 1 \leq 0$ and $k_2^2 - k_2 \leq 0$ hold. As a result,

$$\begin{aligned} \int_0^t \left(q_1^2 x_1^2 + q_2^2 x_2^2\right) dt &\leq \int_0^t \left(k_1 z_1^2 + k_2 z_2^2\right) dt \\ &\leq \gamma \int_0^t \|d\|^2 dt + \tilde{\Theta} \end{aligned}$$

which illustrates (2) holds.

So far, the objectives i)-iii) have been achieved and the main result is summarised as Theorem 1.

Theorem 1: Consider the nonlinear TCSC system (1), if initial condition satisfies $|x_1(0)| < \rho(0)$ and $V(0) \leq p$ with $p > 0$ being a given constant, then the generator rotor angle is SGPFS and other signals of the close-loop systems are bounded with virtual controllers (17) and (20), filters (18) and (21), the adaptive law (33) and the control input u (23).

Remark 7: It is worth emphasizing that the finite-time design process given above has the following two attributes: a) the problem on "the explosion of terms" is avoided because of the dynamic surface control; b) by utilizing the PFTF, the controller design process is simpler than those in [13]–[15]. In addition, the settling time T_f in this work does not depend on the initial condition and designed parameters and can be set to an arbitrary value, which indicates that there exists a convergent time T_f which is smaller than that in [1]–[12]. Besides, in our work, all the adopted control techniques such as practical finite-time control, H_∞ and dynamic surface control can be used in high-order systems. Therefore, the corresponding stability analysis results are also available in fourth or higher order systems.

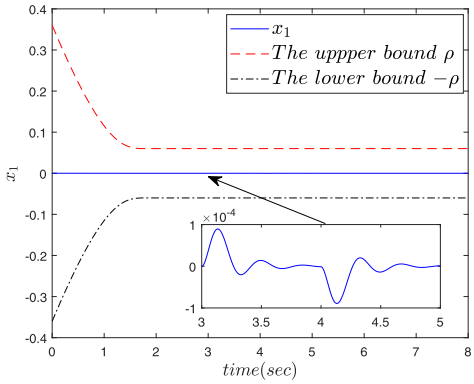

FIGURE 2. The response of x_1.

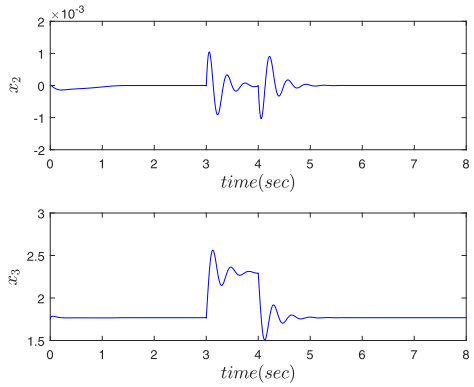

FIGURE 3. The response of x_2 and x_3.

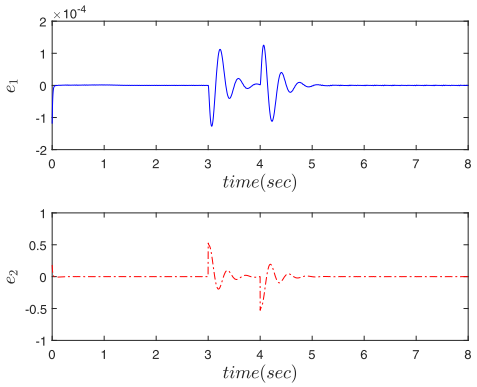

FIGURE 4. The curves of the boundary layer errors.

VI. SIMULATION RESULTS

In this section, simulation experiment is carried out to verify the effectiveness of the proposed method by using Matlab software. Meanwhile, two fault situations are also considered in this section, one is recoverable mechanical fault and the other is unrecoverable mechanical fault. First, the physical parameters and design parameters are given as follows

$$\begin{aligned} &\omega_s = 1, \quad M = 7, \ P_m = 0.9, \ E_q^{'} = 1.067, \ V_s = 0.995, \\ &T_{\text{tcsc}} = 0.05, \quad q_1 = 0.3, \ q_2 = 0.4, \ k_1 = 0.01, \ k_2 = 10, \\ &k_3 = 10, \quad \gamma_1 = 1, \ \gamma_2 = 1, \ \tau_1 = 0.01, \ \tau_2 = 0.05, \\ &\rho_0 = 0.3, \rho_{T_f} = 0.06, \ T = 2, \\ &x(0) = [0.0001, 0, 1.75]^{\mathrm{T}}, \ \theta(0) = [0, 1.75, 0]^{\mathrm{T}}. \end{aligned}$$

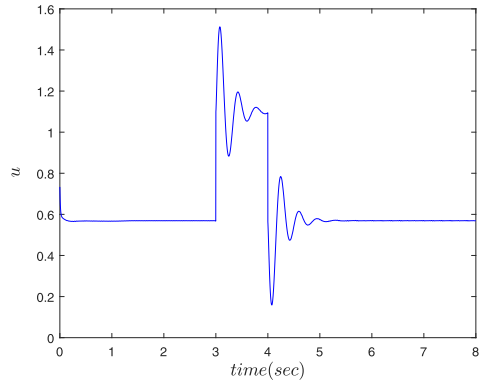

FIGURE 5. The trajectory of the control input u.

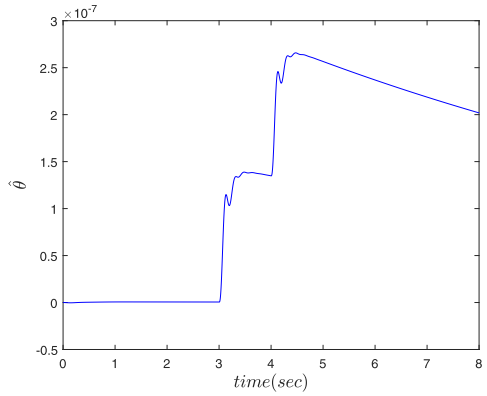

FIGURE 6. The adaptive law $\hat{\theta}$.

According the designed scheme introduced in Section IV and the above-given parameters, the simulation results are shown in the following subsections with two different faults.

A. MECHANICAL FAULT (RECOVERABLE)

In this case, the mechanical fault occurs and it can be recovered. It is assume that a 25% disturbance existed in the mechanical power between $t = 3$ s and $t = 4$s. At this time, the parameter P_m is changed to $\bar{P}_m = (1 + \Delta) P_m$ and

$$\Delta = \begin{cases} 0, & 0\text{s} \le t < 3\text{s} \\ 0.25, & 3\text{s} \le t < 4\text{s} \\ 0, & t > 4\text{s} \end{cases}$$

The simulation results are plotted in Figs. 2-6. It follows from Fig. 2 that the generator rotor angle satisfies the pre-set transient and steady-state properties and it converges to a pre-given small zone in finite-time. It can be seen from Fig. 3 that the states x_2 and x_3 are bounded. The errors e_1 and e_2 approach a small neighbourhood of zero, which can be observed in Fig. 4. The trajectories of the control input signal u and adaptive law $\hat{\theta}$ are shown in Figs. 5 and 6. It is obvious that the proposed method has the certain disturbance rejection ability.

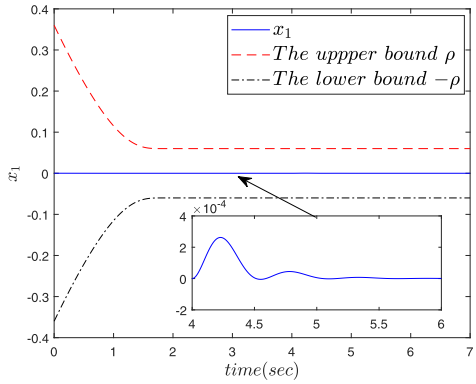

FIGURE 7. The response of x_1.

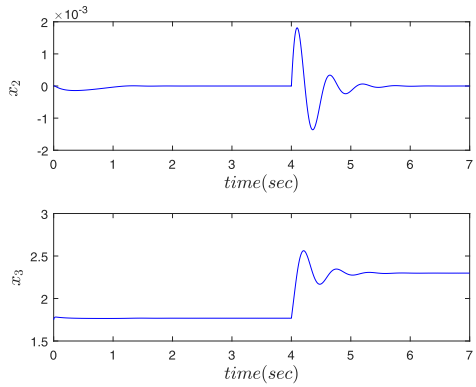

FIGURE 8. The response of x_2 and x_3.

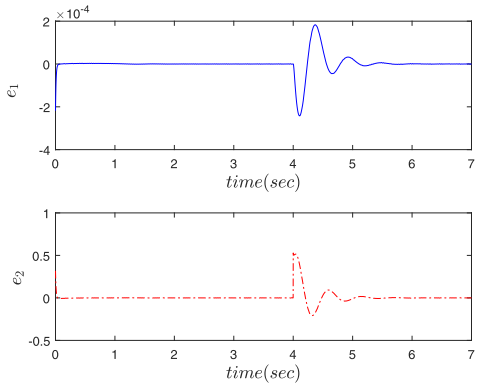

FIGURE 9. The curves of the boundary layer errors.

B. MECHANICAL FAULT (UNRECOVERABLE)

It is worth noting that another mechanical fault, which cannot be recovered, is considered in this subsection, that is

$$\Delta = \begin{cases} 0, & 0\text{s} \le t \le 4\text{s} \\ 0.25, & t > 4\text{s} \end{cases}$$

The corresponding results can be found in Figs. 7-12. It is easy to see that the states x_i with $i = 1, 2, 3$ are bounded and x_1 meets the performance of the pre-assigned time convergence in Figs. 7-8. It can be observed from Fig. 9 that the boundary layer errors e_1 and e_2 are also

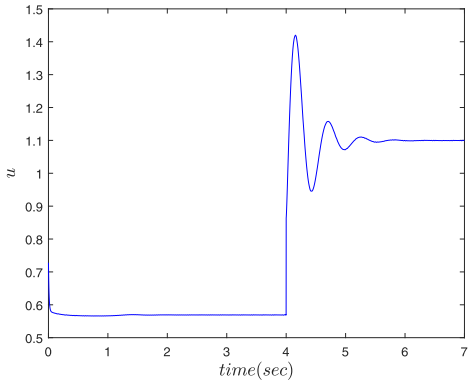

FIGURE 10. The trajectory of the control input u.

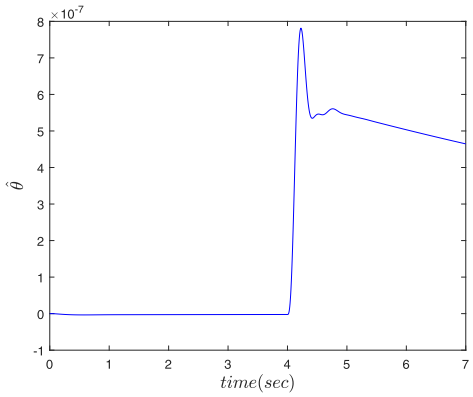

FIGURE 11. The adaptive law $\hat{\theta}$.

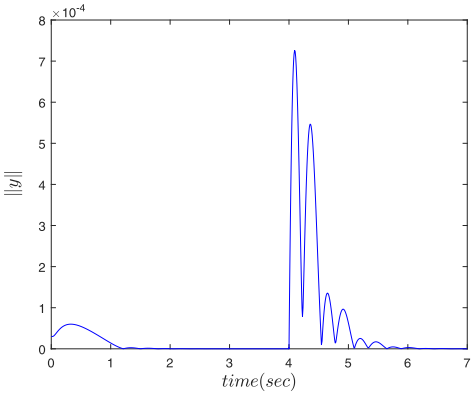

FIGURE 12. The norm of the output $\|y\|$.

bounded. The changing curves of the control input u and adaptive law $\hat{\theta}$ are reported in Figs. 10 and 11. When the fault happens, the presented scheme makes sure that the influence of disturbances on the output is attenuated to a given degree, which can be known from Fig. 12.

Remark 8: The above-mentioned two mechanical faults are different, one is recoverable and the other is unrecoverable, which can be obviously seen from Figs. 3, 5, 7 and 9. Specifically, when the fault is recoverable, it is worth noting in Figs. 3 and 5 that the states and control input recover the originally steady-state case if the fault is cut off. However, these signals will approach a new steady-state value when the fault is unrecoverable, whose results are shown in Figs. 8 and 10.

VII. CONCLUSION

A semi-globally practical finite-time stability (SGPFS) problem has been addressed from a new point of view for the TCSC power system, and a preassigned finite-time function (PFTF) is used. With the aid of PFTF, H_∞ and DSC, a less-complex control design procedure has been provided, which indicates that the proposed method in this note is simpler to be implemented. Besides, it has been proven that the proposed controller guarantees the control objectives of this work. The effectiveness and superiority of the presented technique is illustrated by simulation studies. In future, the practical finite-time control will be studied for multi-machine system. Besides, the idea of the decentralized control for expanding construction systems in [34] can be considered to study the online expansion of large-scale power systems.

REFERENCES

[1] W. L. Li, "Study on the nonlinear adaptive robust control for power systems," Ph.D. dissertation, Dept. College Inf. Sci. Eng., Northeastern Univ., Shenyang, China, 2003.
[2] M. Ishimaru, R. Yokoyama, G. Shirai, and T. Niimura, "Robust thyristor-controlled series capacitor controller design based on linear matrix inequality for a multi-machine power system," *Int. J. Electr. Power Energy Syst.*, vol. 24, no. 8, pp. 621–629, Oct. 2002.
[3] G. Taranto and J. Chow, "A robust frequency domain optimization technique for tuning series compensation damping controllers," *IEEE Trans. Power Syst.*, vol. 10, no. 3, pp. 1219–1225, Aug. 1995.
[4] K. Son and J. Park, "On the robust LQG control of TCSC for damping power system oscillations," *IEEE Trans. Power Syst.*, vol. 15, no. 4, pp. 1306–1312, Nov. 2000.
[5] Y. Sun, Q. Liu, Y. Song, and T. Shen, "Hamiltonian modelling and nonlinear disturbance attenuation control of TCSC for improving power system stability," *IEE Proc.-Control Theory Appl.*, vol. 149, no. 4, pp. 278–284, Jul. 2002.
[6] N. Jiang, B. Liu, J. Kang, Y. Jing, and T. Zhang, "The design of nonlinear disturbance attenuation controller for TCSC robust model of power system," *Nonlinear Dyn.*, vol. 67, no. 3, pp. 1863–1870, Feb. 2012.
[7] J. Fu, J. X. Feng, and J. Zhao, "Novel adaptive backstepping method for TCSC control," *Control Decis.*, vol. 21, no. 10, pp. 1163–1171, 2006.
[8] G. Naresh, M. R. Raju, and S. Narasimham, "Coordinated design of power system stabilizers and TCSC employing improved harmony search algorithm," *Swarm Evol. Comput.*, vol. 27, pp. 169–179, Apr. 2016.
[9] M. Bakhshi, M. H. Holakooie, and A. Rabiee, "Fuzzy based damping controller for TCSC using local measurements to enhance transient stability of power systems," *Int. J. Electr. Power Energy Syst.*, vol. 85, pp. 12–21, Feb. 2017.
[10] A. Halder, N. Pal, and D. Mondal, "Transient stability analysis of a multimachine power system with TCSC controller—A zero dynamic design approach," *Electr. Power Energy Syst.*, vol. 97, pp. 51–71, 2018.
[11] P. Dahiya, V. Sharma, and R. Naresh, "Optimal sliding mode control for frequency regulation in deregulated power systems with DFIG-based wind turbine and TCSC-SMES," *Neural Comput. Appl.*, vol. 31, no. 7, pp. 3039–3056, Jul. 2019.
[12] C. O. Maddela and B. Subudhi, "Robust wide-area TCSC controller for damping enhancement of inter-area oscillations in an interconnected power system with actuator saturation," *Int. J. Electr. Power Energy Syst.*, vol. 105, pp. 478–487, Feb. 2019.
[13] S. P. Bhat and D. S. Bernstein, "Finite-time stability of continuous autonomous systems," *SIAM J. Control Optim.*, vol. 38, no. 3, pp. 751–766, Jan. 2000.
[14] X. Huang, W. Lin, and B. Yang, "Global finite-time stabilization of a class of uncertain nonlinear systems," *Automatica*, vol. 41, no. 5, pp. 881–888, May 2005.

[15] Y. Cheng, H. Du, Y. He, and R. Jia, "Finite-time tracking control for a class of high-order nonlinear systems and its applications," *Nonlinear Dyn.*, vol. 76, no. 2, pp. 1133–1140, Apr. 2014.
[16] S. Huang and Z. Xiang, "Finite-time stabilization of switched stochastic nonlinear systems with mixed odd and even powers," *Automatica*, vol. 73, pp. 130–137, Nov. 2016.
[17] S. Huang and Z. Xiang, "Finite-time stabilization of a class of switched stochastic nonlinear systems under arbitrary switching," *Int. J. Robust. Nonlinear Control*, vol. 26, no. 10, pp. 2136–2152, Jul. 2016.
[18] H. Wang, B. Chen, C. Lin, Y. Sun, and F. Wang, "Adaptive finite-time control for a class of uncertain high-order non-linear systems based on fuzzy approximation," *IET Control Theory Appl.*, vol. 11, no. 5, pp. 677–684, Mar. 2017.
[19] W. Lin and C. Qian, "Adding one power integrator: A tool for global stabilization of high-order lower-triangular systems," *Syst. Control Lett.*, vol. 39, no. 5, pp. 339–351, Apr. 2000.
[20] Y. Hong, "Finite-time stabilization and stabilizability of a class of controllable systems," *Syst. Control Lett.*, vol. 46, no. 4, pp. 231–236, Jul. 2002.
[21] Y. Hong, J. Huang, and Y. Xu, "On an output feedback finite-time stabilization problem," *IEEE Trans. Autom. Control.*, vol. 46, no. 2, pp. 305–309, 2001.
[22] Y. Song, Y. Wang, J. Holloway, and M. Krstic, "Time-varying feedback for regulation of normal-form nonlinear systems in prescribed finite time," *Automatica*, vol. 83, pp. 243–251, Sep. 2017.
[23] Y. Wang and Y. Song, "Leader-following control of high-order multi-agent systems under directed graphs: Pre-specified finite time approach," *Automatica*, vol. 87, pp. 113–120, Jan. 2018.
[24] D. Swaroop, J. K. Hedrick, P. P. Yip, and J. C. Gerdes, "Dynamic surface control for a class of nonlinear systems," *IEEE Trans. Autom. Control*, vol. 45, no. 10, pp. 1893–1899, Oct. 2000.
[25] J. Ma, Z. Zheng, and P. Li, "Adaptive dynamic surface control of a class of nonlinear systems with unknown direction control gains and input saturation," *IEEE Trans. Cybern.*, vol. 45, no. 4, pp. 728–741, Apr. 2015.
[26] Y. Li, S. Tong, and T. Li, "Adaptive fuzzy output feedback dynamic surface control of interconnected nonlinear pure-feedback systems," *IEEE Trans. Cybern.*, vol. 45, no. 1, pp. 138–149, Jan. 2015.
[27] X. Zhang, R. Wang, Y. Fang, B. Li, and B. Ma, "Acceleration-level pseudo-dynamic visual servoing of mobile robots with backstepping and dynamic surface control," *IEEE Trans. Syst. Man Cybern, Syst.*, vol. 49, no. 10, pp. 2071–2081, Oct. 2019.
[28] C. P. Bechlioulis and G. A. Rovithakis, "Adaptive control with guaranteed transient and steady state tracking error bounds for strict feedback systems," *Automatica*, vol. 45, no. 2, pp. 532–538, Feb. 2009.
[29] M. Chen, X. Liu, and H. Wang, "Adaptive robust fault-tolerant control for nonlinear systems with prescribed performance," *Nonlinear Dyn.*, vol. 81, no. 4, pp. 1727–1739, Sep. 2015.
[30] Y. Li, S. Tong, L. Liu, and G. Feng, "Adaptive output-feedback control design with prescribed performance for switched nonlinear systems," *Automatica*, vol. 80, pp. 225–231, Jun. 2017.
[31] W. Si, X. Dong, and F. Yang, "Adaptive neural prescribed performance control for a class of strict-feedback stochastic nonlinear systems with hysteresis input," *Neurocomputing*, vol. 251, pp. 35–44, Aug. 2017.
[32] Y. Liu, X. Liu, Y. Jing, X. Chen, and J. Qiu, "Direct adaptive preassigned finite-time control with time-delay and quantized input using neural network," *IEEE Trans. Neural Netw. Learn. Syst.*, to be published, doi: 10.1109/tnnls.2019.2919577.
[33] Y. Liu, X. P. Liu, and Y. W. Jing, "Adaptive practical preassigned finite-time stability for a class of pure-feedback systems with full state constraints," *Int. J. Robust Nonlinear Control*, vol. 29, no. 10, pp. 2978–2994, Jul. 2019.
[34] Y. Liu, X. P. Liu, Y. W. Jing, H. Q. Wang, and X. H. Li, "Annular domain finite-time connective control for large-scale systems with expanding construction," *IEEE Trans. Syst., Man, Cybern., Syst.*, to be published, doi: 10.1109/TSMC.2019.2960009.

LING CHANG was born in Xingcheng, Liaoning, China. She is currently pursuing the Ph.D. degree with Northeastern University, Shenyang, China.

She is also an Associate Professor and the Deputy Director of the Department of Information and Control Engineering, Shenyang Urban Construction University, Shenyang, China. Her current research interests include stability analysis of nonlinear systems, prescribed performance control, and control problems in power systems.

YANG LIU received the Ph.D. degree in control theory and control engineering from Northeastern University, Shenyang, China, in 2019.

He was a Visiting Scholar with the Department of Electrical Engineering, Lakehead University, Thunder Bay, ON, Canada, from 2016 to 2018. He is currently a Postdoctoral Researcher with the School of Automation, Guangdong University of Technology, Guangzhou, China. His current research interests include finite-time control for nonlinear systems, control problems in modern communication network systems, prescribed performance control, and multiagent systems control and its applications.

YUANWEI JING received the B.S. degree in mathematics from Liaoning University, China, in 1981, and the M.S. and Ph.D. degrees in automatic control from Northeastern University, Shenyang, China, in 1984 and 1988, respectively.

From 1998 to 1999, he was a Senior Visiting Scholar with the Computer Science Telecommunication Program, University of Missouri, Kansas City. He is currently with the School of Information Science and Engineering, Northeastern University. His current research interests include control problems in modern communication network systems, networks traffic management, analysis and control, control of flight craft, and analysis and control of large-scale complex nonlinear systems.

XIANGYONG CHEN received the master's and Ph.D. degrees in control theory and control engineering from the Northeastern University, Shenyang, China, in 2008 and 2012, respectively.

From 2016 to 2017, he was a Visiting Scholar with the Department of Electrical Engineering, Yeungnam University, Gyeongsan, South Korea. His current research interests include complex dynamic system and complex networks, differential game and optimal control, and synchronization control of chaotic systems.

JIANLONG QIU (Member, IEEE) received the Ph.D. degree from Southeast University, Nanjing, China, in 2007.

He was a Visiting Scholar with the Stevens Institute of Technology, Hoboken, NJ, USA, and the University of Rhode Island, Kingston, RI, USA, where he was involved in collaborative research. He is currently a Professor and the Deputy Director of the Department of Research Administration, Linyi University, Linyi, China. His current research interests include genetic networks, stability theory, neural networks, and applied mathematics.